Environ Sci Pollut Res (2016) 23:24846–24856
DOI 10.1007/s11356-016-7722-x

RESEARCH ARTICLE

Characteristics of uranium biosorption from aqueous solutions on fungus *Pleurotus ostreatus*

Changsong Zhao[1,2] · Jun Liu[2] · Hong Tu[2] · Feize Li[2] · Xiyang Li[1] · Jijun Yang[2] · Jiali Liao[2] · Yuanyou Yang[2] · Ning Liu[2] · Qun Sun[1]

Received: 25 July 2016 / Accepted: 15 September 2016 / Published online: 23 September 2016

Abstract Uranium(VI) biosorption from aqueous solutions was investigated in batch studies by using fungus *Pleurotus ostreatus* biomass. The optimal biosorption conditions were examined by investigating the reaction time, biomass dosage, pH, temperature, and uranium initial concentration. The interaction between fungus biomass and uranium was confirmed using Fourier transformed infrared (FT-IR), scanning electronic microscopy energy dispersive X-ray (SEM-EDX), and X-ray photoelectron spectroscopy (XPS) analysis. Results exhibited that the maximum biosorption capacity of uranium on *P. ostreatus* was 19.95 ± 1.17 mg/g at pH 4.0. Carboxylic, amine, as well as hydroxyl groups were involved in uranium biosorption according to FT-IR analysis. The pseudo-second-order model properly evaluated the U(VI) biosorption on fungus *P. ostreatus* biomass. The Langmuir equation provided better fitting in comparison with Freundlich isotherm models. The obtained thermodynamic parameters suggested that biosorption is feasible, endothermic, and spontaneous. SEM-EDX and XPS were additionally conducted to comprehend the biosorption process that could be described as a complex process involving several mechanisms of physical adsorption, chemisorptions, and ion exchange. Results obtained from this work indicated that fungus *P. ostreatus* biomass can be used as potential biosorbent to eliminate uranium or other radionuclides from aqueous solutions.

Keywords Uranium · Biosorption · *Pleurotus ostreatus* · Bioremediation

Responsible editor: Georg Steinhauser

✉ Ning Liu
nliu720@scu.edu.cn

✉ Qun Sun
qunsun@scu.edu.cn

[1] Key Laboratory of Biological Resources and Ecological Environment of the Ministry of Education, College of Life Sciences, Sichuan University, Chengdu 610064, People's Republic of China

[2] Key Laboratory of Radiation Physics and Technology, Ministry of Education, Institute of Nuclear Science and Technology, Sichuan University, Chengdu 610064, People's Republic of China

Introduction

The rapidly expanding nuclear industry all over the world results in the production of enormous amount of radioactive waste. Uranium, a toxic and weakly radioactive heavy metal that has been extensively released into the environment through a great deal of activities related to the storage of radioactive wastes and nuclear industry, can lead to environmental surface and water contamination (Bayramoglu et al. 2015; Bayramoglu and Arica 2016; Sun et al. 2015, 2016; Zhang et al. 2015). Water contaminated by uranium poses great menace to human, animal, and ecological health because it usually has strong toxicity, long half-life, and persistency (Davies and Mazumder 2003). Uranium can be ingested by human beings who may encounter severe health problems even at low concentrations, such as liver and kidney injury, and even lead to death (Schnug and Lottermoser 2013). Therefore, it is of significant importance to remove uranium from water.

The radionuclides and heavy metals can be removed from waste water by lots of methods, which consist of physical, chemical, and biological methods such as ion exchange, membrane filtration, chemical precipitation, oxidation, solvent extraction, electrochemical techniques, and adsorption (Gao et al. 2015; Massoudinejad et al. 2016; He et al. 2016; Saleh 2015; Morocho-Jácome et al. 2016). Compared with other

technologies, adsorption is more efficient, environmental friendly, and easy to handle (Du et al. 2016; Jiang et al. 2016; Chao et al. 2014; Saravanan et al. 2013). Besides, adsorption method contains enormous advantages due to its low cost and wide range of material sources (Kesraoui et al. 2016; Lee et al. 2016; Tiwari et al. 2013). What is more, many researchers have been paying attention to using adsorption methods especially under the condition of low concentrations of heavy metals and radionuclides (Acheampong et al. 2013; Fomina and Gadd 2014). Usually, the biosorbent surface morphology, surface area, and functional groups that are attached to the biosorbent surface have a great effect on the biosorption efficiency (Ali et al. 2016). A variety of adsorbents have been extensively produced and applied to remove radionuclides and heavy metals (Fomina and Gadd 2014). The primary categories of adsorbents comprise activated carbon and synthetic polymers as well as silica-based adsorbents (Jung et al. 2013; Dhir 2014). Although these adsorbents have excellent performance, most of them have been turned out to suffer from the drawback of their high cost, which already became a very serious problem (Ali et al. 2016). Fortunately, many kinds of naturally available, low-cost, and effective biosorbents including microbial sources, leaf-based biosorbent, water hyacinth chitosan, tea leaves, sunflower hulls, activated olive bagasse, calcined oyster shells, banana peels, cedar sawdust, and some types of macro-fungus have been utilized as biosorbent for eliminating metal and dyes from waste water in recent years (Alidoust et al. 2015; Bampaiti et al. 2015; Ertugay and Bayhan 2010; Ramakrishna et al. 2015; Vijayaraghavan and Yun 2008; Vimala and Das 2009; Witek-Krowiak 2012; Zheng et al. 2014). In particular, macro-fungus is regarded as the greatly available natural biosorbents, because macro-fungus grows abundantly and can be planted in various parts of the world. On the other hand, they are large with big biomass as well as tough texture and own other physical traits, which help them be developed into biosorbent without the demand of treatment or immobilization by exclusively bioreactor structure (Nagy et al. 2014; Vimala and Das 2009). Meanwhile, macro-fungus are more suitable to eliminate radionuclides from effluent than other microbes because they have great tolerance for radionuclides and other negative conditions including high cell wall binding ability, extreme pH and efficient metal absorptive capacity (Sarı and Tuzen 2009a). For example, the biosorption capacity of Pb and Cd by the fungus *Amanita rubescens* biomass was found to be 38.4 and 27.3 mg/g at pH 5.0, respectively, which was much higher than that by microbes (Sarı andTuzen 2009b). The maximum biosorption capacity of macro-fungus (*Inonotus hispidus*) towards As(III) and As(V) was very high, which was calculated to be 51.9 and 59.6 mg/g under optimal conditions of pH 6.0 and 2.0 value, respectively (Sarı andTuzen 2009b). However, despite various potential fungous biosorbents have been investigated, little information is available on fungus *P. ostreatus* biomass applied to uranium(VI) biosorption from aqueous solutions.

Pleurotus ostreatus was chosen in this work as it is one of the most common edible fungus in China and also in many other countries. This edible fungi is widely cultivated, toxic-free, renewable, eco-friendly natural sources, and its biomass is cheap and easily available (Yargıç et al. 2015). In this work, the influences of a variety of biosorption factors such as biomass dosage, contact time, uranium concentration, and pH value on biosorption behavior of uranium were studied by batch experiments. The characteristics and mechanism of uranium biosorption on *P. ostreatus* biomass were studied by using Fourier transformed infrared (FT-IR) spectroscopy, scanning electronic microscopy (SEM), X-ray photoelectron spectroscopy (XPS) technique as well as energy dispersive X-ray (EDX) analysis. Furthermore, biosorption process of uranium on *P. ostreatus* was described by using kinetic and equilibrium, as well as thermodynamic data.

Material and methods

Preparation of the biosorbent

The fungus biomass of *P. ostreatus* was purchased from the local market (Chengdu, China). Fungus *P. ostreatus* was washed with tap water and cut into small pieces, and then the dust and impurities were eliminated by using distilled water. The fungus biomass of *P. ostreatus* was dehydrated at 70 °C for 48 h and granulated in a clean mortar to achieve powder. This natural powder was utilized as the biosorbent, which was further stored in a desiccator.

Solutions

All chemicals and reagents were analytical reagent grade. $UO_2(NO_3)_2{\cdot}6H_2O$ was used for uranium stock solution (1 g/L), HNO_3 solution was used for adjusting the pH of the stock solution in order to keep the stock solution in the acidic condition. While working solutions were acquired by proper dilution of prepared stock solution.

Batch biosorption experiments

All uranium biosorption experiments on *P. ostreatus* were performed under ambient conditions, unless otherwise specified. Solutions used in this biosorption experiments were prepared in distilled water. The batch experimental approaches were carried out as follows: NaOH solution and negligible HNO_3 were used to adjust pH values of uranium stock solution firstly. Then 0.05 g *P. ostreatus* powder was added to 20 mL uranium solution. The batch experiments of uranium biosorption on fungus *P. ostreatus* biomass were conducted in Erlenmeyer flasks in an

incubated shaker (150 rpm), which was operated until the reaction achieved equilibrium at given temperature. Biosorption experiments were conducted in triplicate. The suspension was centrifuged (10,000×*g*, 5 min) after reaction and UV spectrophotometer with arsenazo(III) method was used to measure uranium ions concentrations (Zhao et al. 2016).

The biosorption efficiency R (%) and biosorption capacity Q (mg/g) of uranium biosorption on biomass were calculated from the following equations as:

$$R = \frac{C_0 - C_e}{C_0} \times 100\% \quad (1)$$

$$Q = \frac{(C_0 - C_e) \times V}{W} \quad (2)$$

where C_0 and C_e are the initial and concentrations of uranium left in solutions (mg/L), respectively. While V (L) is the volume of the uranium solution and W (g) is the dry weight of the *P. ostreatus* biomass powder. The results were shown as averages through the three repeat experiments.

SEM-EDS analyses

Samples of original fungus *P. ostreatus* (control) and uranium-loaded *P. ostreatus* were studied by SEM. The control and uranium-loaded samples which were dried by using gold sputtering treatment and then installed on stubs for observing the scanning electron microscopy and EDX analysis (S4800, Hitachi, Japan).

Fourier transformed infrared spectroscopy

FT-IR was employed to clarify the functional groups that potentially participated in the biosorption process. In all biosorption experiments, a fungus biomass of 0.05 g was added to a plastic centrifuge tube containing 20 ml 10 mg L^{-1} U(VI) solution at pH 4 value. The mixtures were cultured in incubator for 6 h at 30 °C, and samples of original fungus *P. ostreatus* (control) were prepared without adding uranium ions, then regained by centrifugation (5000 rpm, 20 min) and lyophilized. All prepared samples were finally used for analysis using the standard KBr method. The FT-IR spectra were acquired over the range of 4000–400 cm^{-1} by using a FT-IR spectrometer (Thermo, Nicolet 6700).

X-ray photoelectron spectroscopy

XPS technique was a valuable spectroscopic tool, which was applied to investigate the uranium biosorption process and analyze biomass surface composition, chemical-state alterations, as well as the mechanism of the interaction between uranium and fungus *P. ostreatus* biomass. The original *P. ostreatus* and uranium-loaded *P. ostreatus* biomass were handled under optimal conditions. The lyophilized samples were used for X-ray photoelectron spectroscopy by using the Al Kα line with an Axis-Ultra instrument (SAM800, Kratos, UK). X-ray photoelectron spectroscopy chamber was conducted at 10–9 Torr. The instrument was setup at 20 eV pass energy, and the experimental detecting resolution was expected to be 0.65 eV.

Data analysis

Mean and standard deviation values of three replicates in this work were calculated. SPSS 17.0 software was applied to statistics and analyzes the experimental data, where it was possible to assess whether the investigated influencing factors were significant corresponding to the experimental error. All statistics were performed by using the Origin 8.0 (USA).

Results and discussion

Batch biosorption studies

The influence of different biosorption factors like contact time, biosorbent dosage, and initial uranium concentrations as well as pH value on removal efficiency are optimized in this section, which are routinely applied to determine the appropriate biosorption conditions for the uranium uptake by fungus *P. ostreatus* biomass are discussed comprehensively.

The contact time played a vital role in the biosorption between fungus *P. ostreatus* biomass and uranium. As displayed in Fig. 1a, the biosorption efficiency of *P. ostreatus* biomass increased with the increase of reaction time and then achieved equilibrium until 6 h. The biosorption ability was in the state of dynamic balance that has certain amount of U(VI) biosorbed from fungus *P. ostreatus* biomass on this point. After that, there is no remarkable increase in the biosorption efficiency of uranium ions, because the surface pores of *P. ostreatus* biomass may be covered, besides, it encounters more challenges for uranium to get into the interior of the biomass pores. In order to ensure that enough reaction time was reached, biosorption tests were further carried out for 12 h. Thus, the reaction time of all subsequent biosorption experiments was chosen as 6 h.

The biosorbent dosage was also a comparatively important parameter which could significantly limit the biosorption capacity. As shown in Fig. 1b, the effect of *P. ostreatus* dosage on uranium removal efficiency was determined by changing biosorbent dosage of *P. ostreatus* at the range from 0 to 12.5 g/L. It was evidently observed that uranium removal efficiency increased from 0 to 86.28 ± 1.18 % with increase in biomass dose of 0–7.5 g/L of fungus *P. ostreatus* biomass. These results are attributed to the fact that the biosorption sites are still not unsaturated in the process. The increasing biosorbent dosage can provide more area on surface and the availability sites

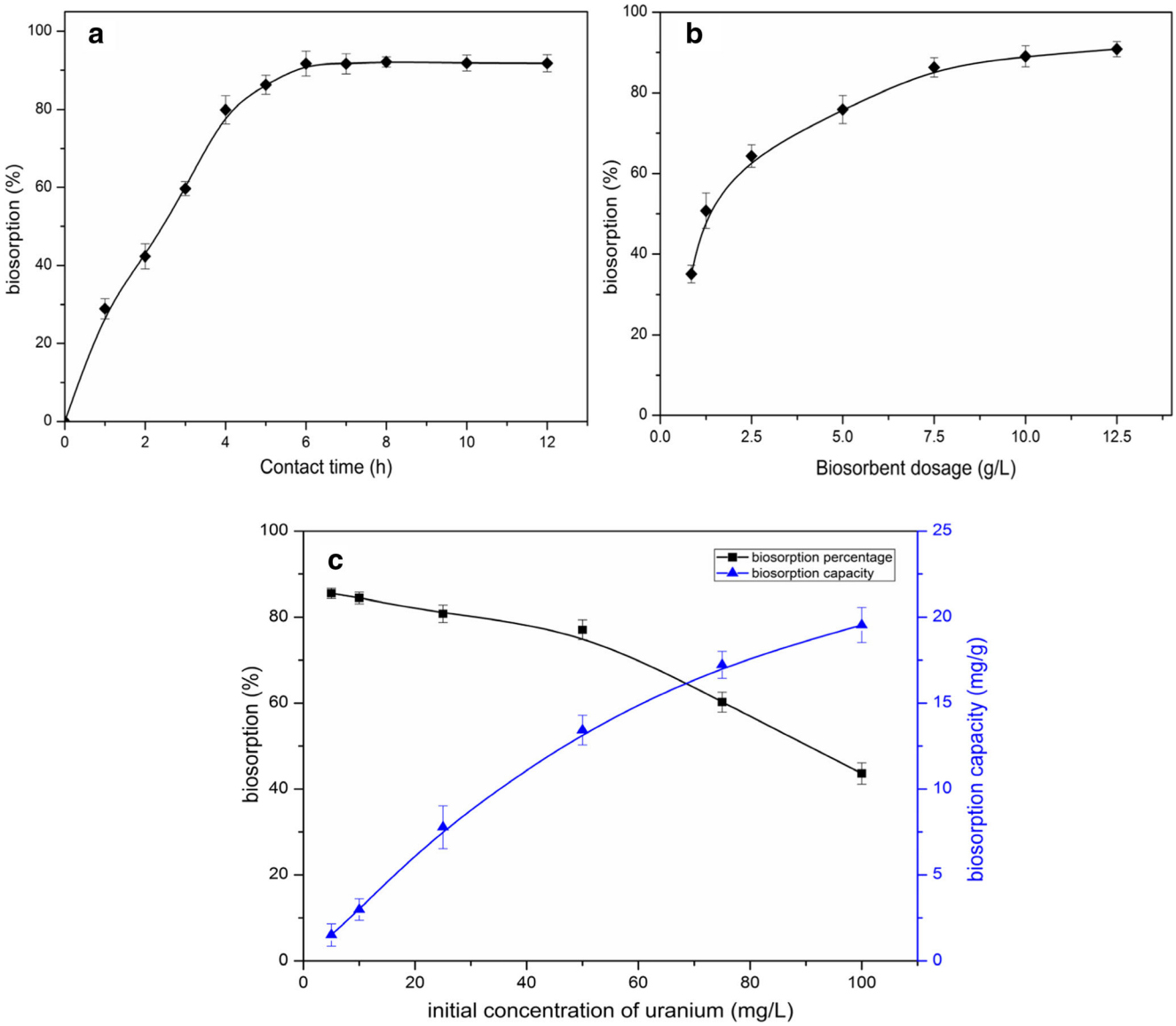

Fig. 1 Effect of **a** contact time, **b** biosorbent dosage, **c** initial concentration of uranium on U(VI) biosorption by *Pleurotus ostreatus* biomass (pH 4.0; agitation speed = 150 rpm; temperature, 25 °C)

of biomass (Sarı &Tuzen 2009a). The removal efficiency of uranium reached a maximum value of 90.81 ± 1.52 %, and then became mild significant because the amount of uranium left in final solution was very low. Therefore, the results implied that a dose of 7.5 g/L of *P. ostreatus* could be adequate for the removal of uranium.

Uranium biosorption on fungus *P. ostreatus* is obviously influenced by the initial uranium concentration in aqueous solutions. The biosorption tests were employed to determine the impact of uranium concentration by varying it from 5 to 100 mg/L, and results were exhibited in Fig. 1c. The results showed that with the increase of uranium concentration from 5 to 100 mg/L, the removal efficiency decreases from 85.48 ± 1.03 to 43.61 ± 0.94 %. The proportion of the initial moles of uranium that was available for biomass surface was exceedingly low when at lower concentration of the uranium, and then the remaining biosorption was not dependent on uranium concentration. At higher concentration of uranium ions, however, the available sites which were used for biosorption became fewer by comparison with the moles of uranium ions and hence the biosorption efficiency of uranium would rely on the initial uranium concentration. Similar results obtained in previous research have been reported for biosorption of cadmium using heartwood powder (*Areca catechu*) biomass from aqueous solution (Chakravarty et al. 2010). For the 10-mg/L of initial uranium concentration, the optimum value of U(VI) biosorption efficiency using *P. ostreatus* biomass was found to be 84.48 ± 1.31 %.

pH value was also an important and sometimes even dominant factor that had a great impact on the biosorption ability of

radionuclide by biomass, because it had an effect on protonation and deprotonation of functional groups attached to the fungus surface, and it could determine the uranium speciation in solution (Ahmad et al. 2014). The effect of pH on uranium biosorption by *P. ostreatus* biomass was studied at 30 °C through the change of pH in uranium solution. The pH value ranging from 2.0 to 7.0 was chosen here, because it could avoid uranyl ion complexation caused by high pH value. The highest value of biosorption efficiency 90.67 ± 0.9 % was observed when pH was 4.0, as presented in Fig. 2a. Furthermore, the chemical speciation for U(VI) in Fig. 2b was for an extra-pure aqueous solution, soluble U(VI) species like UO_2^{2+} predominated in the uranium solution below pH 4.0 according to the distribution of uranium species, which was computed by using visual MINTEQ 3.0. Consequently, the biosorption experiments for uranium by *P. ostreatus* biomass in this study were conducted at pH 4.0, because the uranium solution speciation at pH 4.0 was dominated by UO_2^{2+}.

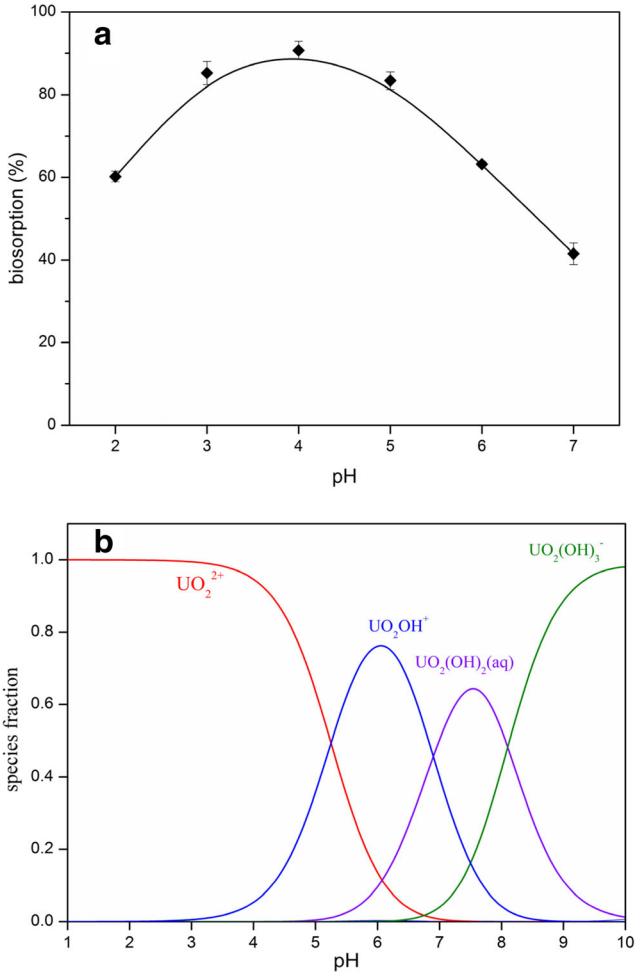

Fig. 2 Effect of pH on the biosorption of U(VI) by *Pleurotus ostreatus* biomass (biosorbent dosage, 0.05 g; U concentration, 10 mg/L; contact time = 6 h; agitation speed = 150 rpm; temperature, 25 °C)

SEM-EDX analyses

SEM is the most common utilized characterization techniques that can be used for investigating the surface morphology and porosity as well as texture morphology of fungus biosorbent. As exhibited in Fig. 3, SEM micrographs and EDX spectra were obtained before and after uranium ion biosorption on *P. ostreatus* biomass. Fungus *P. ostreatus* has obvious micro-porous structure, which can provide a high specific surface area (Fig. 3a, c). It could be clearly observed from SEM pictures that the *P. ostreatus* biomass became rough surface and full of impurities on the surface of the fungus *P. ostreatus* saturated with uranium (Fig. 3b, d) than in terms of before biosorption. This observation was further demonstrated by EDX analysis which illustrated U(VI) peaks in the spectrum (Fig. 3f) while such a peak could not be observed on the original fungus *P. ostreatus* surface (Fig. 3e). In addition, there is a decrease of potassium peak after the biosorption, which can be explained by the possibility of ion exchange. Besides, a similarly decreased peak of thorium was reported in the previous biosorption research (Ding et al. 2014).

FT-IR spectroscopy

The FT-IR is a helpful technique to illuminate the functional groups which participate in U(VI) binding of biosorption by *P. ostreatus*. The FT-IR spectra were observed in the total range between 4000 and 400 cm^{-1} in this work, and the spectra of *P. ostreatus* for uranium-free (control) and uranium-treated samples were presented in Fig. 4. The FT-IR spectrum of fungus *P. ostreatus* exhibited a large amount of peaks in biosorption, suggesting its complexity in natural biomass. Moreover, it also confirmed distinct surface properties and changes in functional groups of *P. ostreatus* biomass. In general, the transference of these functional group bands and intensity were remarkably altered after uranium biosorption on *P. ostreatus*.

Some characteristic peaks can be assigned to the involvement of the main functional groups that are presented in the *P. ostreatus* biomass based on the examination of highly complex IR spectra. The complex biosorption from 2900 to 3000 cm^{-1} are associated with the asymmetric vibration of C–H bond of the $–CH_2$ integrated with the $–CH_3$ groups (Ahmed et al. 2014). The spectra for uranium-accumulated samples exhibited a miner shift in the position of the 2856.07–2864.49 cm^{-1} compared with original biomass, which was related to the N–H bending oscillation of secondary amide II band (−CONH–) (Chen andYang 2006). In case of uranium-treated samples, the peak position at 1657.56 cm^{-1} was attributed to C=O stretching vibration and amide I band. The peak at 1544.39 cm^{-1} was attributed to a shift associating with the –NH stretching and the –CN bending vibration (Kazy et al. 2009). A peak at 1457.01 cm^{-1} region was observed in control samples due to the presence of carboxyl group. After uranium biosorption, the peak of spectra exhibited a change at

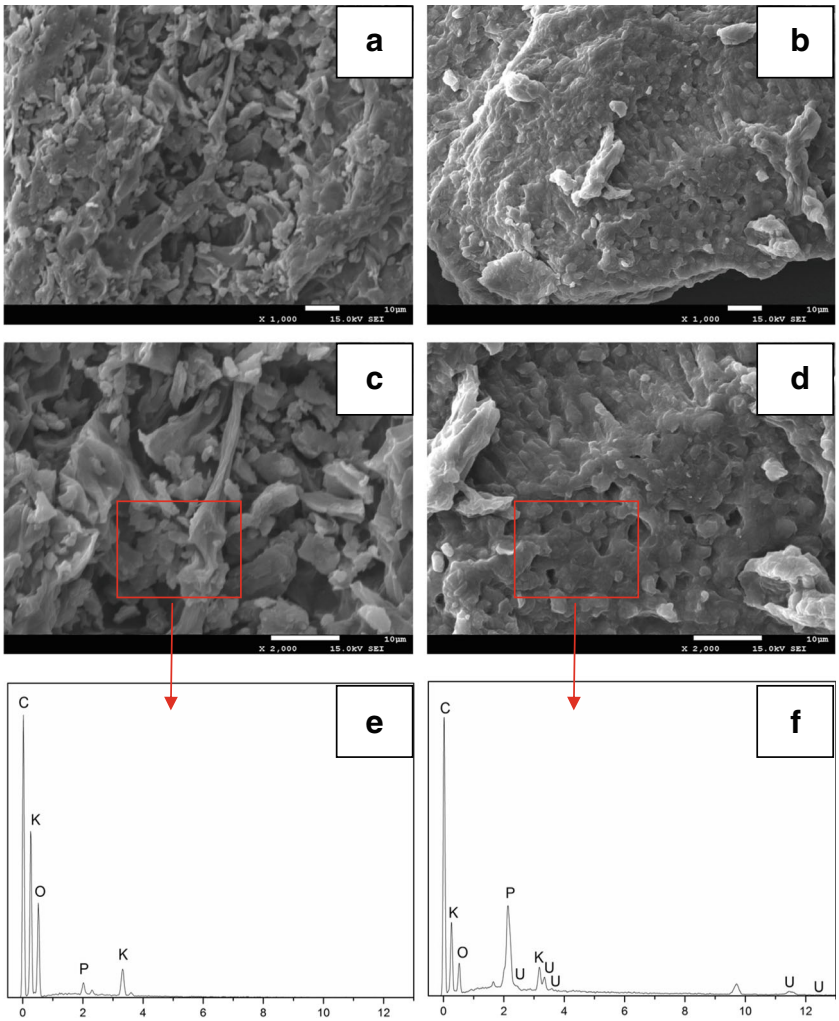

Fig. 3 SEM images and EDS analyses of *Pleurotus ostreatus* before (**a**, **c**) and after U biosorption (**b**, **d**), respectively

1409.35 cm^{-1} further implying the stretching vibration characteristic of $–CH_2$ motion or $–CH_3$ anti-symmetrical. A minor change of the peak observed at 1370.09–1376.11 cm^{-1} which was attributed to the symmetric bending COO– vibration, most likely revealed the status of carboxyl groups binding with uranium. And there has a shift from 1252.35 to 1255.14 cm^{-1} in comparison with the control samples, which implies the binding of uranium with phosphate groups. Especially, a new peak at 915.89 cm^{-1} was observed and was caused by the asymmetrical stretching vibration of UO_2^{2+}.

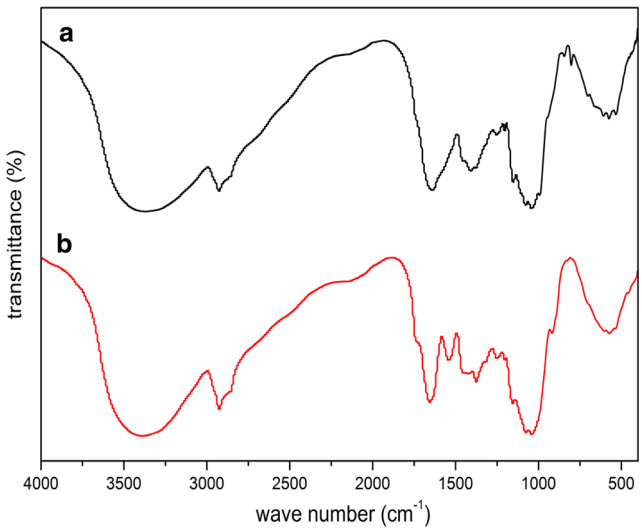

Fig. 4 FT-IR spectrum of *Pleurotus ostreatus* biomass: **a** before and **b** after uranium biosorption

Therefore, the FT-IR analysis reveals that several functional groups presented on the surface of the fungus *P. ostreatus* biomass are able to bind with uranium ions during the U (VI) biosorption procedure.

X-ray photoelectron spectroscopy analysis

XPS was performed to investigate chemical-state alterations and mechanism for uranium biosorption on fungus *P. ostreatus* biomass (Regenspurg et al. 2009). The elemental composition of biomass samples achieved from XPS investigation is calculated in Table 1. The original biomass and uranium-loaded *P. ostreatus* samples were analyzed by

Table 1 Elemental composition of control and uranium-loaded *Pleurotus ostreatus* samples were determined by X-ray photoelectron spectroscopy

Element component (%)	Control	Uranium-loaded sample
C	71.25	72.47
O	25.57	24.53
N	2.41	1.98
P	0.77	0.78
U	–	0.24

XPS, which consisted of C1s, O1s, and U4f spectrum (Fig. 5). As the wide scan data exhibited in Fig. 5a, a new peak assigned to the asymmetrical vibration of the UO_2^{2+} was observed after the procedure of biosorption, indicating that uranium had been biosorbed on the *P. ostreatus* biomass via chemical binding. Particularly, U4f XPS spectrum was shown in Fig. 5d, it is obvious that two special peaks with a binding energy at 381.493 eV and 392.070 eV were assigned to U4f7/2 as well as U4f5/2, respectively (Zhao et al. 2016). It is critical to focus on the higher-resolution spectra so as to comprehend the electronic states of the elements. Compared with the C1s spectrum of uranium-free biomass samples (Fig. 5b), the peak at 287.265 eV is O–C–O or C=O C–(O, N), at 285.942 eV as well as at 284.778 eV of C–(C, H) were slightly shifted in the uranium-loaded biomass samples, C1s spectrum showed a direct proof that amide and carboxylate was main functional groups which was interacted with uranium. In particular, the peaks of O=C–OR and O=C–OH at 288.79 binding energy (eV) disappeared because of carboxyl or ester functions, which was well in accordance with our FT-IR results. Two peaks (531.957 and 533.063 eV) were observed from the O1s peaks in control *P. ostreatus* biomass samples, which could be assigned to O=P, O=C, and C–O–C, respectively. This O1s spectra result was consistent with the carbon groups in previous studies. Accordingly, XPS analysis indicated that uranyl ions were bonded to different functional groups of fungus *P. ostreatus* biomass and the biosorption was dependent on complexation process.

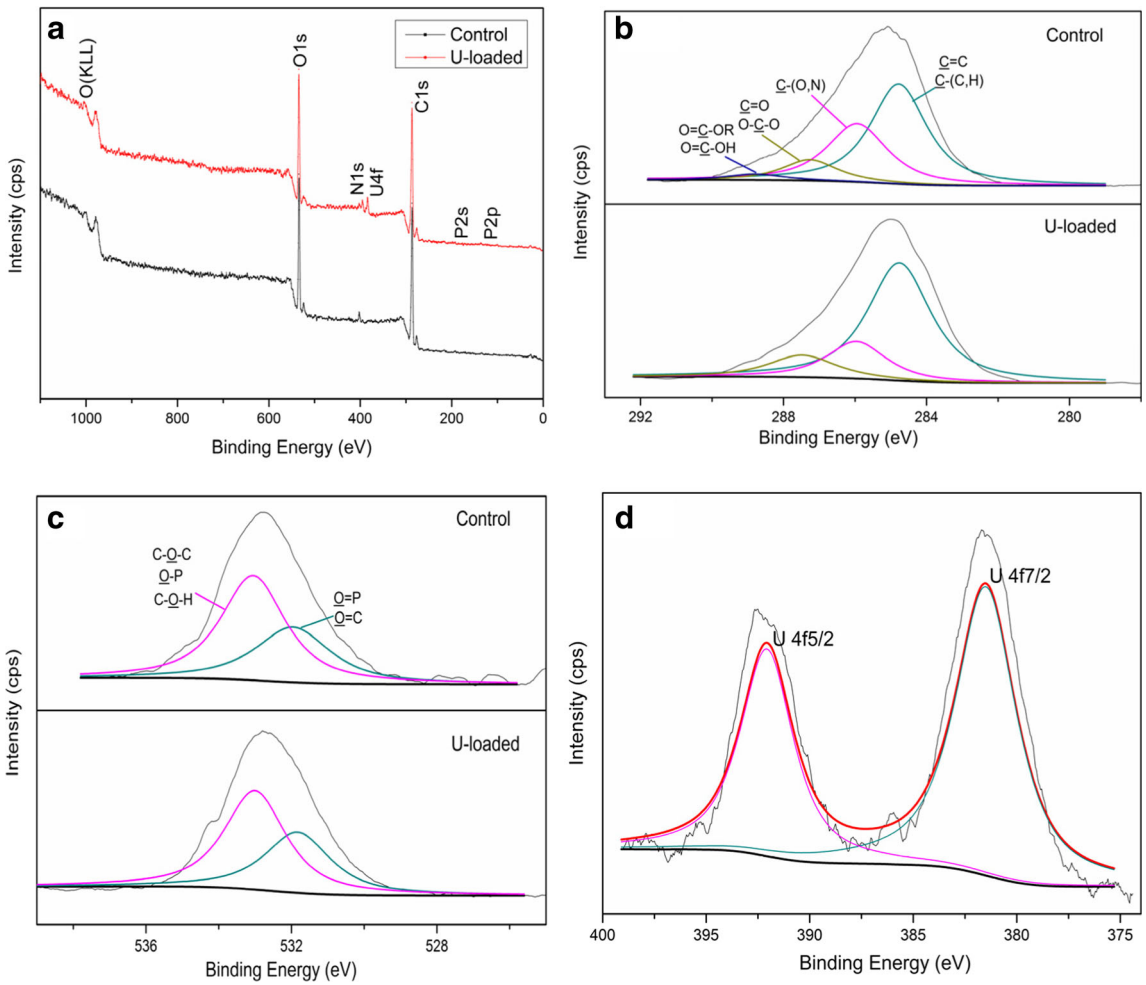

Fig. 5 XPS Intensity curves of U(VI) biosorption on fungus *Pleurotus ostreatus* biomass: **a** total survey scans, **b** C 1 s, **c** O 1 s, and **d** U 4f as a function of the binding energy

Table 2 The first-order and the second-order kinetics for uranium biosorption by *Pleurotus ostreatus* biomass

First-order kinetics			Second-order kinetics		
k_1 (min^{-1})	q_e (mg g^{-1})	R^2	k_2 (mg g^{-1} min^{-1})	q_e(mg g^{-1})	R^2
0.761 ± 0.088	5.06 ± 0.565	0.8794	0.4283 ± 0.047	4.77 ± 0.007	0.9898

Adsorption kinetics

Adsorption kinetics can evaluate the rate of the uranium biosorption at the solid-solution interface and can provide meaningful information when studying the mechanisms and reaction characteristics. Pseudo-first and pseudo-second-order kinetic models that were employed to identify U(VI) biosorption kinetic by fungus *P. ostreatus* biomass. The linear form of the pseudo-first-order kinetic is known as the Lagergren equation and is represented as (Zare et al. 2015):

$$\ln(q_e - q_t) = \ln q_e - k_1 t \quad (3)$$

where q_t and q_e are the uranium ions biodsorbed at time t and equilibrium (mg/g), respectively, and k_1 (min^{-1}) is the reaction equilibrium constant of the first-order equation. The pseudo-second-order kinetic model utilized in uranium biosorption study is calculated by following equation (Ferrer-Polonio et al. 2016):

$$\frac{t}{q_t} = \frac{1}{k_2 q_e^2} + \left(\frac{1}{q_e}\right) t \quad (4)$$

where k_2 (g mg^{-1} min^{-1}) is the reaction rate equilibrium constant of second order.

These kinetic models were applied to speculate possible mechanism of uranium biosorption on fungus *P. ostreatus* biomass. The values of k_1, k_2, and q_e are calculated in Table 2. As exhibited in Fig. 6a, b, uranium biosorption were superbly suitable for pseudo-second-order kinetic by contrast to pseudo-first-order kinetic which has a relative high correlation coefficient. The pseudo-second-order kinetic is also in accordance with chemisorption which involved in the valency force by means of the sharing electrons between biomass and uranium (Mal et al. 2016). These results implied that biosorption on *P. ostreatus* biomass is a complex process, which may relate to several mechanisms such as physical adsorption, chemisorptions, as well as ion exchange. Moreover, these results suggested that chemisorption is the main rate-limiting factor in uranium biosorption on *P. ostreatus* biomass.

Adsorption isotherms

The association between the biomass and the uranium concentrations from aqueous has been namely evaluated by using Langmuir and Freundlich isotherm models at equilibrium. At the same time, the Langmuir biosorption isotherm was helpful for investigating heavy metal biosorption and was the most extensively utilized isotherm for the biosorption of a solute from aqueous solutions. The linear form of the Langmuir isotherm is calculated by using the following equation (Yargıç et al. 2015):

$$\frac{C_e}{q_e} = \frac{1}{k_L q_m} + \frac{C_e}{q_m} \quad (5)$$

where C_e (mg/L) is the equilibrium uranium concentration, q_e (mg/g) is the equilibrium uranium removal by biomass, q_m is the maximum biosorption capacity (mg/g), and k_L is the Langmuir constant (L/mg) which is relevant to the connection

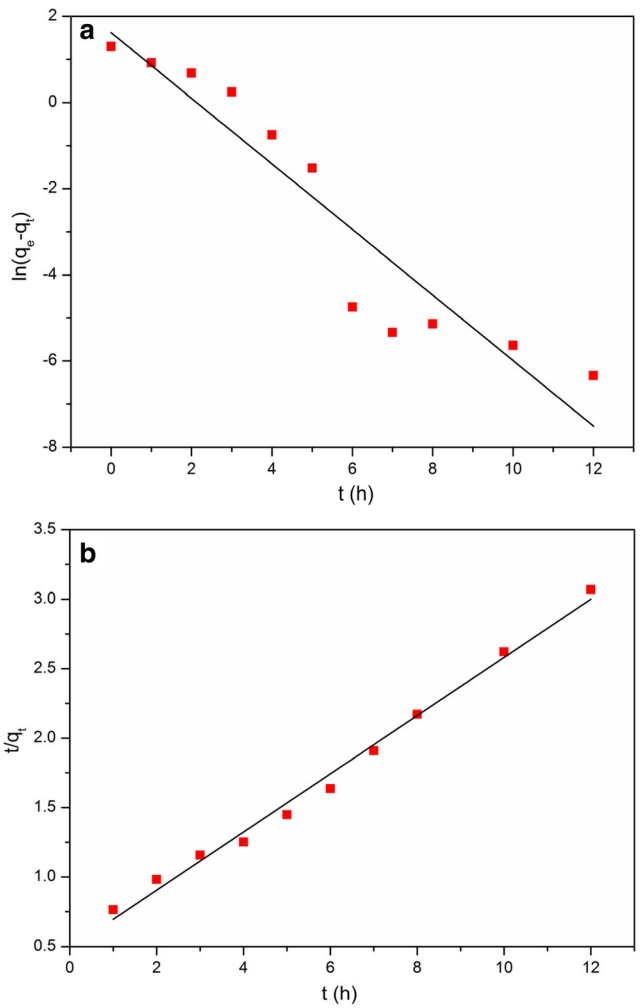

Fig. 6 Pseudo-first-order kinetic plot (**a**) and pseudo-second-order kinetic plot (**b**) for uranium biosorption by *Pleurotus ostreatus* biomass, respectively

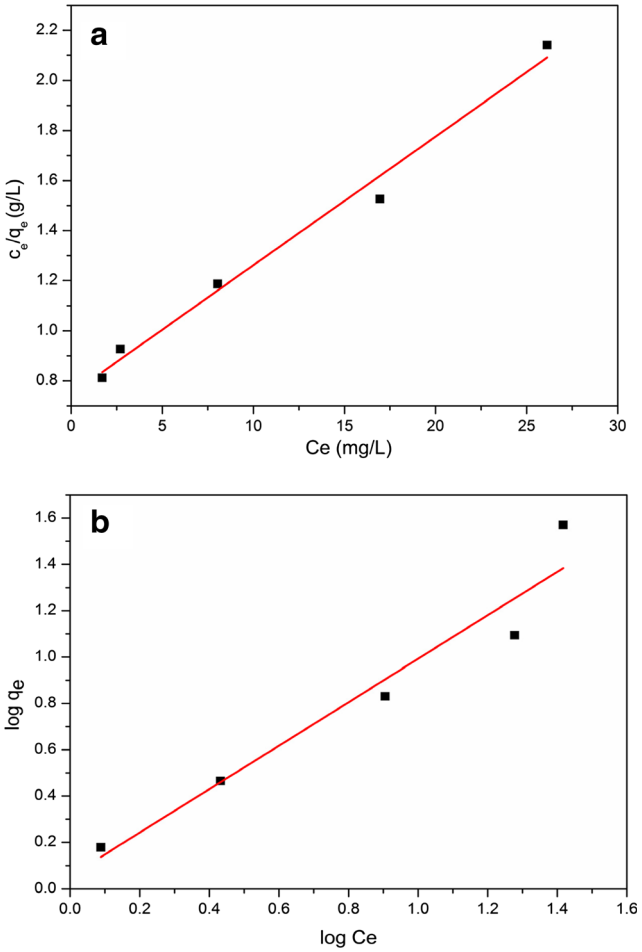

Fig. 7 **a** Langmuir and **b** Freundlich isotherms of uranium biosorption on *Pleurotus ostreatus* biomass, respectively

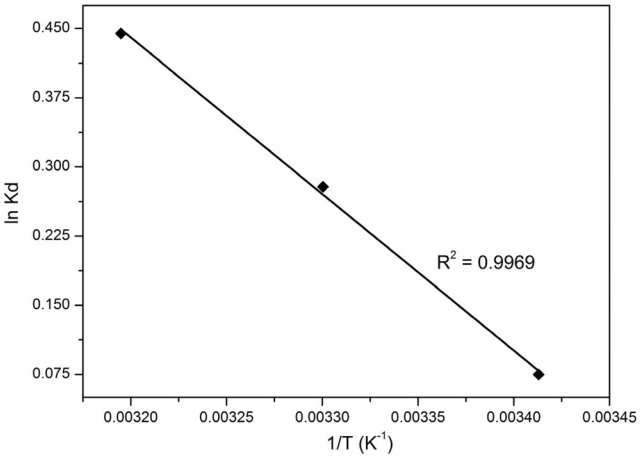

Fig. 8 The thermodynamics for the biosorption of uranium on fungus *Pleurotus ostreatus* biomass

of biomass binding sites, the constant is associated with the energy of the biosorption.

The experimental U(VI) uptake values which were obtained in this study have also been determined by the Freundlich model. And the Freundlich isotherm model is available to multilayer biosorption on heterogeneous *P. ostreatus* biomass surface where there is no consolidated distribution of biosorption heat. Freundlich isotherm can be expressed by (Bayramoglu and Yakup Arica 2009; Ting et al. 2016):

$$\log q_e = \frac{1}{n_f}\log C_e + \log k_f \quad (6)$$

where n_f and k_f are Freundlich constants associated with biosorption intensity and biosorption capacity, respectively. The plot of $\log q_e$ versus $\log C_e$ was used to achieve the Freundlich constants k_f and n_f, which could provide a slope of $1/n_f$ as well as intercept of $\log k_f$. Langmuir constants q_m (mg/g) and k_L (L/mg) were determined by slope and the intercept of the plot of C_e/q_e value versus C_e (Fig. 7a), respectively. Besides, the slope and the intercept of $\log q_e$ versus $\log C_e$ plot were used to acquire Freundlich equation constants and correlation coefficient (Fig. 7b). The acquired Langmuir as well as Freundlich isotherm parameters are summarized in Table 3. It is noteworthy that these biosorption parameters are more suitable for Langmuir model than the Freundlich model according to correlation coefficient R^2 (0.9838) value. The Langmuir model predicted the formation of the adsorbed uranium monolayer, while there are no side interactions with the biosorbed uranium assuming the biosorption of one uranium per binding site on the homogeneous *P. ostreatus* biomass surface. This indicates that the governing mechanism is chemisorption with distinct possibility of monolayer biosorption of uranium occurring on the surface of the *P. ostreatus* biomass. It has been extensively developed that the Langmuir biosorption isotherm presumes that biosorption occurs at specific sites within the biomass. Thus, once the uranium ions dominate a site on the surface of biomass, no further biosorption will take place at that site.

Adsorption thermodynamics

The spontaneity and heat change of uranium biosorption on *P. ostreatus* biomass were estimated by determining the thermodynamic parameters. The biosorption potential of *P. ostreatus* biomass for U(VI) removal was estimated at the

Table 3 Parameters of the Langmuir and Freundlich isotherms for the biosorption of uranium on *Pleurotus ostreatus* biomass

Langmuir isothern			Freundlich isotherm		
q_m (mg/g)	K_L (L/mg)	R^2	n_f	K_f (mg/g)	R^2
19.44 ± 0. 48	0.069 ± 0.003	0.9838	1.066 ± 0.129	1.134 ± 0.133	0.9238

Table 4 The thermodynamic parameters for the sorption of uranium on *Pleurotus ostreatus* biomass

$\Delta G°$ (kJ/mol)			$\Delta H°$ (kJ/mol)	$\Delta S°$ (J mol^{-1} K^{-1})	Standard deviations
293 K	303 K	303 K			
−0.182	−0.702	−1.157	14.11	48.81	±0.223

temperatures of 20, 30, as well as 40 °C. In order to assess thermodynamic behavior of U(VI) biosorption on fungus *P. ostreatus* biomass, thermodynamic data such as the change in entropy ($\Delta S°$), free energy ($\Delta G°$), and enthalpy ($\Delta H°$) were estimated by following equations (Yargıç et al. 2015):

$$\Delta G° = -RT\ln K_d \quad (7)$$

where, R is the general gas constant, and the value is 8.314 J^{-1} mol^{-1} K, K_d (q_e/c_e) is the distribution coefficient, and T (K) is reaction temperature. The enthalpy ($H°$) and entropy ($S°$) parameters were expressed as (Gao et al. 2015):

$$\ln K_d = \frac{\Delta S°}{R} - \frac{\Delta H°}{RT} \quad (8)$$

The experimental results illustrated biosorption of uranium by *P. ostreatus* biomass was depended upon the temperature. The slope of a plot of ln K_d and intercept of $1/T$ are employed to identify $\Delta H°$ and $\Delta S°$ parameters (Fig. 8). The values of $\Delta H°$, $\Delta S°$, as well as $\Delta G°$ for U(VI) biosorption on *P. ostreatus* biomass are listed in Table 4. The Gibbs free energy implies that if the biosorption of uranium using biomass is spontaneous, then higher negative value reveals that more energy can be in favor of biosorption. The negative values of ($\Delta G°$) for uranium ions indicated that the uranium biosorption on *P. ostreatus* biomass is spontaneous and the $\Delta G°$ value was negative with increasing temperature. These results indicated that higher temperature made the uranium biosorption easier. In addition, the positive values of $\Delta H°$ point out that the biosorption process using *P. ostreatus* biomass is endothermic, indicating the biosorption reaction needs energy and increasing temperature thus promoting the biosorption of U(VI). $\Delta S°$ possesses a positive value that causes increasing randomness at the solid/liquid interface through uranium biosorption on fungus *P. ostreatus* biomass.

Conclusions

This work evaluated the characteristics of fungus *P. ostreatus* biomass used as green and economical biosorbent for uranium biosorption from aqueous solution. The optimum pH of the biosorption is found to be 4, where the uranium biosorption efficiency reaches 91.81 %. The FT-IR analysis revealed that several functional groups presented on the surface of *P. ostreatus* are in charge of the binding of uranium ions, the SEM-EDX and XPS analyses further confirmed the uranium biosorption. Pseudo-second-order model reflected the kinetic experimental parameters in diverse uranium concentrations very well. Equilibrium adsorption exhibited that biosorption obeyed the Langmuir adsorption isotherm better than the Freundlich isotherm model. The biosorption behaviors of uranium using *P. ostreatus* biomass were spontaneous and endothermic according to the investigation of thermodynamic data. Biosorption of uranium involved several mechanisms such as physical adsorption, chemisorptions, as well as ion exchange. The results indicated that fungus *P. ostreatus* biomass can serve as promising biosorbent to remove uranium or other radionuclides from aqueous solutions. Besides, fungus *P. ostreatus* is easily cultivable and inexpensive as well as effective.

Acknowledgments This work was financially supported by China National Natural Science Foundation (grant no. 21071102, 91126013) and the National Fund of China for Fostering Talents in Basic Science (J1210004).

References

Acheampong MA, Pakshirajan K, Annachhatre AP, Lens PNL (2013) Removal of Cu(II) by biosorption onto coconut shell in fixed-bed column systems. J Ind Eng Chem 19:841–848

Ahmad MF, Haydar S, Bhatti AA, Bari AJ (2014) Application of artificial neural network for the prediction of biosorption capacity of immobilized *Bacillus subtilis* for the removal of cadmium ions from aqueous solution. Biochem Eng J 84:83–90

Ahmed SH, El Sheikh EM, Morsy AM (2014) Potentiality of uranium biosorption from nitric acid solutions using shrimp shells. J Environ Radioact 134:120–127

Ali RM, Hamad HA, Hussein MM, Malash GF (2016) Potential of using green adsorbent of heavy metal removal from aqueous solutions: adsorption kinetics, isotherm, thermodynamic, mechanism and economic analysis. Ecol Eng 91:317–332

Alidoust D, Kawahigashi M, Yoshizawa S, Sumida H, Watanabe M (2015) Mechanism of cadmium biosorption from aqueous solutions using calcined oyster shells. J Environ Manag 150:103–110

Bampaiti A, Yusan S, Aytas S, Pavlidou E, Noli F (2015) Investigation of uranium biosorption from aqueous solutions by *Dictyopteris polypodioides* Brown algae. J Radioanal Nucl Chem 307:1335–1343

Bayramoglu G, Arica MY (2016) Amidoxime functionalized *Trametes trogii* pellets for removal of uranium (VI) from aqueous medium. J Radioanal Nucl Chem 307:373–384

Bayramoglu G, Yakup Arica M (2009) Construction a hybrid biosorbent using *Scenedesmus quadricauda* and Ca-alginate for biosorption of Cu(II), Zn(II) and Ni(II): kinetics and equilibrium studies. Bioresour Technol 100:186–193

Bayramoglu G, Akbulut A, Arica MY (2015) Study of polyethyleneimine- and amidoxime-functionalized hybrid biomass of *Spirulina (Arthrospira) platensis* for adsorption of uranium (VI) ion. Environ Sci Pollut Res 22:17998–18010

Chakravarty P, Sarma NS, Sarma HP (2010) Biosorption of cadmium(II) from aqueous solution using heartwood powder of *Areca catechu*. Chem Eng J 162:949–955

Chao H-P, Chang C-C, Nieva A (2014) Biosorption of heavy metals on *Citrus maxima* peel, passion fruit shell, and sugarcane bagasse in a fixed-bed column. J Ind Eng Chem 20:3408–3414

Chen JP, Yang L (2006) Study of a heavy metal biosorption onto raw and chemically modified Sargassum sp. via spectroscopic and modeling analysis. Langmuir 22:8906–8914

Davies J-M, Mazumder A (2003) Health and environmental policy issues in Canada: the role of watershed management in sustaining clean drinking water quality at surface sources. J Environ Manag 68:273–286

Dhir B (2014) Potential of biological materials for removing heavy metals from wastewater. Environ Sci Pollut Res 21:1614–1627

Ding C, Feng S, Cheng W, Zhang J, Li X, Liao J, Yang Y, An Z, Luo S, Yang J, Tang J, Liu N (2014) Biosorption behavior and mechanism of thorium on Streptomyces sporoverrucosus dwc-3. J Radioanal Nucl Chem 301:237–245

Du J, Sun P, Feng Z, Zhang X, Zhao Y (2016) The biosorption capacity of biochar for 4-bromodiphengl ether: study of its kinetics, mechanism, and use as a carrier for immobilized bacteria. Environ Sci Pollut Res 23:3770–3780

Ertugay N, Bayhan YK (2010) The removal of copper (II) ion by using mushroom biomass (*Agaricus bisporus*) and kinetic modelling. Desalination 255:137–142

Ferrer-Polonio E, Mendoza-Roca JA, Iborra-Clar A, Pastor-Alcañiz L (2016) Adsorption of raw and treated by membranes fermentation brines from table olives processing for phenolic compounds separation and recovery. J Chem Technol Biotechnol 91:2094–2102

Fomina M, Gadd GM (2014) Biosorption: current perspectives on concept, definition and application. Bioresour Technol 160:3–14

Gao JK, Hou LA, Zhang GH, Gu P (2015) Facile functionalized of SBA-15 via a biomimetic coating and its application in efficient removal of uranium ions from aqueous solution. J Hazard Mater 286:325–333

He K, Chen Y, Tang Z, Hu Y (2016) Removal of heavy metal ions from aqueous solution by zeolite synthesized from fly ash. Environ Sci Pollut Res 23:2778–2788

Jiang S, Wang X, Yang S, Shi H (2016) Characteristics of simultaneous ammonium and phosphate adsorption from hydrolysis urine onto natural loess. Environ Sci Pollut Res 23:2628–2639

Jung C, Heo J, Han J, Her N, Lee S-J, Oh J, Ryu J, Yoon Y (2013) Hexavalent chromium removal by various adsorbents: powdered activated carbon, chitosan, and single/multi-walled carbon nanotubes. Sep Purif Technol 106:63–71

Kazy SK, D'Souza SF, Sar P (2009) Uranium and thorium sequestration by a *Pseudomonas* sp.: mechanism and chemical characterization. J Hazard Mater 163:65–72

Kesraoui A, Moussa A, Ali GB, Seffen M (2016) Biosorption of alpacide blue from aqueous solution by lignocellulosic biomass: *Luffa cylindrica* fibers. Environ Sci Pollut Res 23:15832–15840

Lee H, Shim E, Yun HS, Park YT, Kim D, Ji MK, Kim CK, Shin WS, Choi J (2016) Biosorption of Cu(II) by immobilized microalgae using silica: kinetic, equilibrium, and thermodynamic study. Environ Sci Pollut Res 23:1025–1034

Mal J, Nancharaiah YV, van Hullebusch ED, Lens PN (2016) Effect of heavy metal co-contaminants on selenite bioreduction by anaerobic granular sludge. Bioresour Technol 206:1–8

Massoudinejad M, Ghaderpoori M, Shahsavani A, Amini MM (2016) Adsorption of fluoride over a metal organic framework Uio-66 functionalized with amine groups and optimization with response surface methodology. J Mol Liq 221:279–286

Morocho-Jácome AL, Sato S, de Carvalho JCM (2016) Ferric sulfate coagulation and powdered activated carbon adsorption as simultaneous treatment to reuse the medium inArthrospira platensiscultivation. J Chem Technol Biotechnol 91:901–910

Nagy B, Măicăneanu A, Indolean C, Mânzatu C, Silaghi-Dumitrescu L, Majdik C (2014) Comparative study of Cd(II) biosorption on cultivated *Agaricus bisporus* and wild *Lactarius piperatus* based biocomposites. Linear and nonlinear equilibrium modelling and kinetics. Journal of the Taiwan Institute of Chemical Engineers 45:921–929

Ramakrishna M, Li XJ, Avner A, Suresh V (2015) Fruit peels as efficient renewable adsorbents for removal of dissolved heavy metals and dyes from water. ACS Sustain Chem Eng 3:1117–1124

Regenspurg S, Schild D, Schäfer T, Huber F, Malmström ME (2009) Removal of uranium (VI) from the aqueous phase by iron (II) minerals in presence of bicarbonate. Appl Geochem 24:1617–1625

Saleh TA (2015) Isotherm, kinetic, and thermodynamic studies on Hg(II) adsorption from aqueous solution by silica- multiwall carbon nanotubes. Environ Sci Pollut Res 22:16721–16731

Saravanan D, Gomathi T, Sudha PN (2013) Sorption studies on heavy metal removal using chitin/bentonite biocomposite. Int J Biol Macromol 53:67–71

Sarı A, Tuzen M (2009a) Kinetic and equilibrium studies of biosorption of Pb(II) and Cd(II) from aqueous solution by macrofungus (*Amanita rubescens*) biomass. J Hazard Mater 164:1004–1011

Sarı A, Tuzen M (2009b) Biosorption of as(III) and as(V) from aqueous solution by macrofungus (*Inonotus hispidus*) biomass: equilibrium and kinetic studies. J Hazard Mater 164:1372–1378

Schnug E, Lottermoser BG (2013) Fertilizer-derived uranium and its threat to human health. Environ Sci Technol 47:2433–2434

Sun Y, Yang S, Chen Y, Ding C, Cheng W, Wang X (2015) Adsorption and desorption of U(VI) on functionalized graphene oxides: a combined experimental and theoretical study. Environ Sci Technol 49: 4255–4262

Sun Y, Zhang R, Ding C, Wang X, Cheng W, Chen C, Wang X (2016) Adsorption of U(VI) on sericite in the presence of *Bacillus subtilis*: a combined batch, EXAFS and modeling techniques. Geochim Cosmochim Acta 180:51–65

Ting TM, Nasef MM, Hashim K (2016) Evaluation of boron adsorption on new radiation grafted fibrous adsorbent containing N-methyl-D-glucamine. J Chem Technol Biotechnol 91:2009–2017

Tiwari JN, Mahesh K, Le NH, Kemp KC, Timilsina R, Tiwari RN, Kim KS (2013) Reduced graphene oxide-based hydrogels for the efficient capture of dye pollutants from aqueous solutions. Carbon 56: 173–182

Vijayaraghavan K, Yun YS (2008) Bacterial biosorbents and biosorption. Biotechnol Adv 26:266–291

Vimala R, Das N (2009) Biosorption of cadmium (II) and lead (II) from aqueous solutions using mushrooms: a comparative study. J Hazard Mater 168:376–382

Witek-Krowiak A (2012) Analysis of temperature-dependent biosorption of Cu2+ ions on sunflower hulls: kinetics, equilibrium and mechanism of the process. Chem Eng J 192:13–20

Yargıç AŞ, Yarbay Şahin RZ, Özbay N, Önal E (2015) Assessment of toxic copper(II) biosorption from aqueous solution by chemically-treated tomato waste. J Clean Prod 88:152–159

Zare K, Sadegh H, Shahryari-ghoshekandi R, Maazinejad B, Ali V, Tyagi I, Agarwal S, Gupta VK (2015) Enhanced removal of toxic Congo red dye using multi walled carbon nanotubes: kinetic, equilibrium studies and its comparison with other adsorbents. J Mol Liq 212: 266–271

Zhang R, Chen C, Li J, Wang X (2015) Investigation of interaction between U(VI) and carbonaceous nanofibers by batch experiments and modeling study. J Colloid Interface Sci 460:237–246

Zhao C, Liu J, Li X, Li F, Tu H, Sun Q, Liao J, Yang J, Yang Y, Liu N (2016) Biosorption and bioaccumulation behavior of uranium on *Bacillus* sp. dwc-2: investigation by box-Behenken design method. J Mol Liq 221:156–165

Zheng S, Huang H, Zhang R, Cao L (2014) Removal of Cr(VI) from aqueous solutions by fruiting bodies of the jelly fungus (*Auricularia polytricha*. Appl Microbiol Biotechnol 98:8729–8736